

Object Shape Retrieval through Grasp Exploration

Diego R. Faria* Jose Prado* Paulo Drews Jr.* Jorge Dias*

* *Institute of Systems and Robotics, Department of Electrical Engineering and Computers, University of Coimbra, Coimbra, Portugal*

Abstract—In this work an approach for object shape retrieval using 3D data acquired from grasp exploration is proposed. The data is acquired from an electromagnetic motion tracking device using one sensor on the thumb and another one on the index fingertip to track the finger movements around the object to obtain its shape. Gaussian Mixture Models (GMM) for points clustering and outliers removal is used. Through GMM is possible to detect features like eigenvalues to represent each shape (e.g. sphere, cylinder and plane) as demonstrated in [11]. After recovering the shape of the object by a probabilistic approach, least square minimization to find the object orientation and scale for its representation is adopted. We are also introducing a preliminary work with stereo camera that aims at acquiring visual information for data fusion (e.g. vision and grasp exploration) to obtain 3D object reconstruction. Calibration results between stereo camera and electromagnetic motion tracking device is presented.

I. INTRODUCTION

Robotics is moving towards the research and development of technologies that permit the introduction of the robots in our daily lives. On the other side, if a robot is supposed to share a human environment, it should be able to cope with the presence of humans and interact with them in a very friendly way. To create such applications some problems need to be solved, including the identification and modeling of human intentions, object perception and grasp strategies. As robots increasingly become part of our everyday lives, they will serve as caretakers for the elderly and disabled, assistants in surgery and rehabilitation, and educational toys. But for this to happen, programming and robot autonomy must become simpler and human-robot interaction more natural. This challenge is particularly relevant to new generation of robots, which must intervene in natural environments, interact with people and operate in human environments. Applications of service robots will require advanced capabilities of grasping objects and skills that allow a robot to recognize the object also through the grasp exploration. Humans use the hand for recognizing some objects properties such as size, texture and etc. Grasp exploration for acquiring object properties is important in robotic field to assist other sensors such as vision and laser in order to obtain more information of an object. Humans use multiple sensory information for recognizing objects. Estimation of object properties can be improved combining information through different cues.

This research aims at developing methods for grasp interpretation and object's characterization based on the

movements of the fingertips around the object. We intend to retrieve the object shape by active touch and as future work we intend to obtain the 3D object reconstruction by fusion of visual cues and grasp exploration. Obtaining the 3D shape is possible to determine the best place to grasp the object through its geometrical properties. Using this knowledge (object representation) is possible to endow a robot to grasp different types of object including unknown objects.

II. RELATED WORK

Several studies have been carried out to obtain haptic information of an object [17], [20]. Some works mention geometric methods for grasp determination. The approach reported in [4], particularly addressed to polygonal shapes, consisting in determining all the regions that guarantee antipodal point grasps through of inscribed circumferences [13]. This approach is not applicable to a work universe of real manufactured objects, without shape restrictions, but the idea of taking distances from the centroid to opposite points in the outer contour, useful to deal with some kinds of symmetry. In [3] the authors have used superquadric functions for shape recovery from haptic exploration with multi-fingered robot hands using fingertip tactile sensors. They have applied a hybrid minimization method utilizing a genetic algorithm by considering the contact normal information to recover superquadric primitives from synthetic exploration data.

In the context of detection of primitive shapes, it is a common task in many areas of geometry related computer science. Along the last decades, a vast number of algorithms has been proposed. Some authors used the well-known Hough's transform to obtain the shape [2], but it has a high computational cost to compute 3D information. Other techniques are based on a region growing [19], which use a seed region in the scan data and is then grown into neighboring areas. In the recent years, some authors have proposed RANSAC-based shape detection method [15], which is a robust method for shape retrieval. A survey about these methods can be found in [16].

III. GRASPING EXPLORATION

A. Scenario and Devices

In our scenario we are using an electromagnetic tracker device, one sensor on the fingertip of the index finger and another one on the thumb. We are acquiring the shape of the object performing movements of these two fingers around the object. The raw data is used by the shape retrieval algorithm (Section IV). Using the two main fingers for grasping (e.g. thumb and index finger) is enough to acquire the object shape. In our experiments we have used a bottle of wine trying

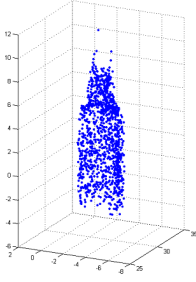


Figure 1. Raw data acquired from the magnetic tracker sensors after the movements of the thumb and index fingers movements around the bottle



Figure 2. Polhemus Liberty tracker device and a glove with sensors attached on each fingertip.

to recover its shape (cylinder). Fig.1 shows the raw data acquired from the two sensors on the fingertips after perform the movements around the bottle.

The motion tracking device Polhemus Liberty [1] has 6 DoF for each sensor, x,y,z coordinates and yaw, pitch and roll information based on sensor's frame of reference. The frame rate of each sensor was defined to work in this scenario with 15Hz. Performing a linear movement of 10cm per second the sensor leads to 0.0221 cm of error. It is roughly a linear scaling so that 100cm per second is about 2mm of error. The resolution position at 30cm range is 0.0004cm and the resolution orientation is 0.0012°. Fig. 2 shows the Polhemus Liberty 240/8 magnetic tracker device and a glove used to attach the sensors on the fingertips.

B. 3D Points Clustering for Outliers Removal

After acquiring the 3D points by grasping exploration the clustering of points facilitates to recover the shape and remove the outliers that are not part of the object. One solution to remove outliers is using the *mixture of Gaussian function*, or *Gaussian Mixture Models (GMM)*.

A GMM is a probability density function described by a convex linear combination of Gaussian density functions [12]. Therefore, a function is a mixture of Gaussian functions if it has the form:

$$f(\mathbf{x}, \Theta) = \sum_{k=1}^K p_k g(\mathbf{x}; \mu_k, \Sigma_k) \quad (\mathbf{x} \in \mathbb{R}^N) \quad (1)$$

where the functions g are Gaussian densities which are defined by $\mu_k \in \mathbb{R}^N$ and Σ_k , means and the covariance matrices, respectively, and the coefficients p_k , known as the *mixing probabilities*, which satisfy:

$$p_k \geq 0 \quad \text{and} \quad \sum_{k=1}^K p_k = 1. \quad (2)$$

In this paper, Θ denotes the $K(1 + N + N^2)$ dimensional vector containing all the parameters of the given Gaussian mixture:

$$\Theta = ((\theta_1, p_1), \dots, (\theta_K, p_K)) \quad (3)$$

where

$$\theta_k = (\mu_k, \Sigma_k) \quad (4)$$

is a vector containing all the coordinates of the means μ_k and all the entries of the covariance matrix Σ_k . The conditions in Eq. (2) guarantee that f is indeed a density function.

Mixtures of Gaussian functions provide good models of clusters of points: each cluster corresponding to a Gaussian density with mean somewhere in the centroid of the cluster, and with a covariance matrix somehow measuring the spread of that cluster. Conversely, given a set of points in \mathbb{R}^N , one can try to find the mixture of Gaussian functions Θ that best fits those points, using a method known as *Expectation Maximization* (see section 2.3 in [12]). This algorithm together with an agglomerative clustering strategy estimate the number of clusters. This estimation is based on the Rissenen order identification criteria known as minimum description length (MDL) [14]. This is equivalent to maximum-likelihood (ML) estimation when the number of clusters is fixed, but in addition it allows the number of clusters to be accurately estimated.

The result of this method is the Gaussian functions and the probability of each point belong to this Gaussian. It allows the outliers removal as well as facilitates the shape retrieval.

IV. RETRIEVAL OF BASIC SHAPES

A. Learning and Classification of Basic Shapes

The shape retrieval is acquired by a probabilistic classification using a Bayesian model. The raw data acquired by grasp exploration is used to find out if the data matches with some basic shapes like sphere, cylinder or a plane. For that, GMM for clustering and outliers removal is used. Using a probabilistic approach we are able to learn and classify the shapes. Given the clustering of the points we compute the features of each known shape. The features extracted are the eigenvalues. From the covariance matrix of each shape we extract three eigenvalues and we normalize these values as follows:

$$e_i = \frac{\lambda_i}{\lambda_{max}} \quad (5)$$

where e represents the normalized eigenvalue; i represents an index for all eigenvalues found for each shape and λ_{max} is the maximum eigenvalue from the three eigenvalues found for each shape. After this normalization step, we keep the maximum and minimum eigenvalues of each shape for the learning phase. We have generated randomly 20.000 synthetic shapes representing sphere, cylinder and plane, all with Gaussian noise. The learning phase is based on histogram techniques, computing a histogram for each shape accumulating all maximum and minimum eigenvalues correspondent to each shape (Fig. 3, 4, 5). To compute a histogram we create a matrix of dimension 100x100. For each observation (a given shape) we extract the normalized eigenvalues and these eigenvalues correspond to the x and y index of the matrix (histogram).

After analyzing all observation for each shape we have 3 histograms. We normalize each histogram and each one represents the training set for classification of shapes. Given a set of observation to represent a type of shape S we have the probability of each feature, E_{max} and E_{min} so that we have $P(E_{max}, E_{min}|S)$. To understand the general classification model some definitions are done as follows:

1. s is a known shape from all possible S (e.g. cylinder, sphere and plane);
2. e_{max} is a certain value of feature, representing maximum normalized eigenvalue;
3. e_{min} is a certain value of feature, representing minimum normalized eigenvalue;

Learning the probability distribution $P(E_{max}, E_{min}|S)$ for each known shape and knowing the priors (uniform distribution) we can apply Bayes rule for the classification:

$$P(s|e_{max}, e_{min}) = \frac{P(e_{max}, e_{min}|s) P(s)}{\sum_j P(e_{max}, e_{min}|s_j) P(s)} \quad (6)$$

After 3000 trials (i.e., 1000 randomly for each shape), the classification model obtained satisfactory results: 97.53%. The problem found during the classification was some confusion with the cylinder and sphere when the diameter of a cylinder was similar to its height so that it was classified as sphere. Sometimes the sphere was classified as cylinder due to noise, it makes the radius varying more than the tolerable. Another case was the cylinder classified as plane, it happens when the cylinder height is close to zero, i.e., when the radius is bigger than the height. These results showed us that even using simulated shapes generated randomly with noise for the learning phase, we obtained good classification with real and synthetic data.

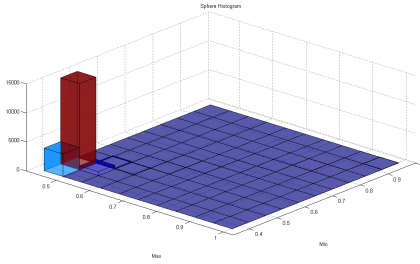


Figure 3. Learned histogram: sphere.

B. Shape Orientation and Scale Matching

After the classification of each shape, to find the disposition of this shape concerning rotation and scale is necessary. For that, we use the algorithm proposed by Núñez *et al* [11] that is used to retrieve the shape in robotic maps. It finds the shape that better approximate to an ideal basic shape from Ψ_{shape} . They use the mathematical space of the Gaussian mixture model which is described by the covariance

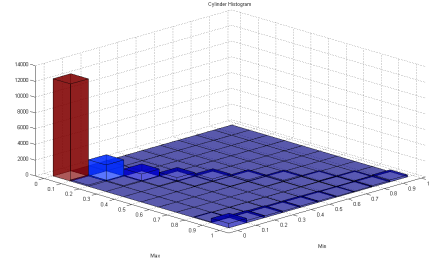


Figure 4. Learned histogram: cylinder

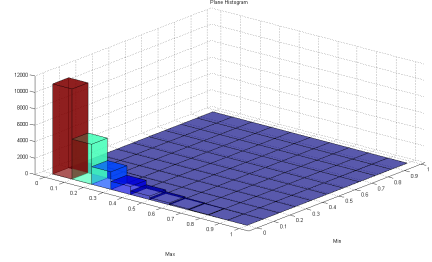


Figure 5. Learned histogram: plane

and mean of the Gaussian functions. The Gaussian mixture associated to the 3D points is denoted as Π . The shape retrieval algorithm is based on the covariance matrices matching. The best model of the shape and the rigid transformation T with respect to an ideal shape is the main idea this algorithm. Gaussian functions are matched with each basic shape which is measured the similarity between their covariance matrices, $d_\Psi = \{d_{sphere}, d_{cylinder}, d_{plane}\}$. The minimum value of d_Ψ determines the shape that best approximates to the cloud of points, just as the rigid transformation.

Covariance matching is a basic task in measurement design [8]. The goal is to obtain a distance measurement of two covariance matrices. The space of covariance matrices is not a vector space and therefore a standard arithmetic difference does not measure the difference between them. But covariance matrices are symmetric and positive semi-definite and then can be formulated a distance based on Riemannian metric. They use the distance metric described by Foerstner and Moonen [8] which is defined as follows:

$$d(\Sigma_1, \Sigma_2) = \sqrt{\sum_{i=1}^N \ln^2 \lambda_i(\Sigma_1, \Sigma_2)} \quad (7)$$

where Σ_1 and Σ_2 are the two input covariance matrices, λ represents the generalized eigenvalues of Σ_1 and Σ_2 , and N is the dimensionality of the matrices. Considering Σ_1 as the covariance of the Gaussian function which identify a shape to be recognized and Σ_2 as the covariance of a basic shape, i.e. sphere, cylinder or plane. To consider possibles rotations and scaling changes of the model, it must be noted that

$$\Sigma_i = T \Sigma_j T^T = (R \cdot L) \Sigma_j (R \cdot L)^T \quad (8)$$

where T represents the Rigid Transformation applied to the ideal geometric shape (neither scaling nor rotation), which is composed of scaling and rotation matrices, R and L .

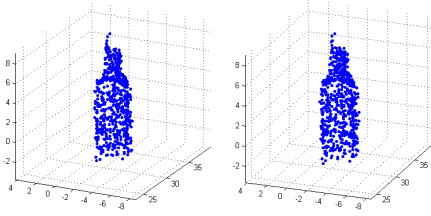


Figure 6. Left image: Raw Data acquired from the finger movements around the bottle. Right image: data with Gaussian noise.

In this approach, the translation is directly known with the mean information of each Gaussian and rotation is the known rotation matrix with three degree of freedom using Euler angles. The matrix L represents the diagonal matrix with scale for each axis. It is possible to minimize Eq. (7) using a least squares minimization method based on Levenberg-Marquardt algorithm, which modifies the rotation and scaling matrices in each iteration. A starting guess of the parameters is required to reduce the number of iterations needed to converge and remove local minima situations. The algorithm uses a good approximation to the rigid transformation T according to the eigenvectors values of the two covariance matrices.

This mentioned method could be used to match the shape beyond of only rotation and scale. However, we are using this method just to match the rotation and scale of each classified shape, since our probabilistic classification using the Bayesian model obtained better results.

V. RESULTS AND FUTURE DIRECTIONS

The movements of the thumb and index finger around the object were performed in 60 seconds. The frame rate of the sensors used on the fingertips for grasp exploration was 15 Hz per second.

Fig.6 shows the raw data and the data with Gaussian noise that were used to test the efficiency of the clustering algorithm.

Fig. 7 shows the result of the GMM. The input of the the first GMM was the raw data and for the second one was the data with Gaussian noise. We can see a small variation in the disposition of the GMM, but the clustering still remains the same. Two cluster were generated for the bottle object for afterwards each cluster represent a shape primitive. Our approach has classified a suitable shape to represent the object and the algorithm used for rotation and scale recovered the shape disposition. It demonstrates that our shape recovering approach works well even with noisy data.

Fig. 8 shows the raw data acquired through the contour following exploratory procedure, the GMM generated from the 3D points and the recovered shape. From each Gaussian we could recovery the shape by classification. By using the least square minimization method we could find the orientation and scale for each shape primitive among the known basic shapes (cylinder, plane and sphere). For this object (bottle of wine) the algorithm easily recovered the cylinder shape for each one of the two Gaussians, as well as the scale in x, y, z axes and the rotation in Euler angles.

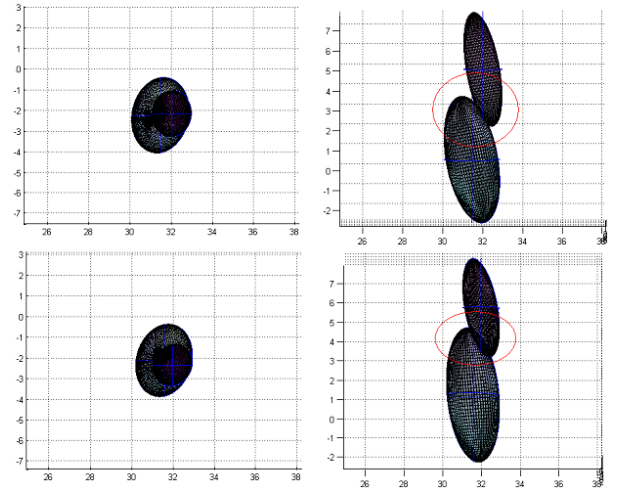


Figure 7. Top-left: superior view of the GMM generated from raw data; Top-right: Lateral view of The GMM generated from the raw data; Down-Left: Superior view of the GMM generated with Gaussian noise; Down-right: Lateral view of the GMM generated from the data with Gaussian noise. The red circles in the lateral views show the region that presents different dispositions in the GMM (due to noise data).

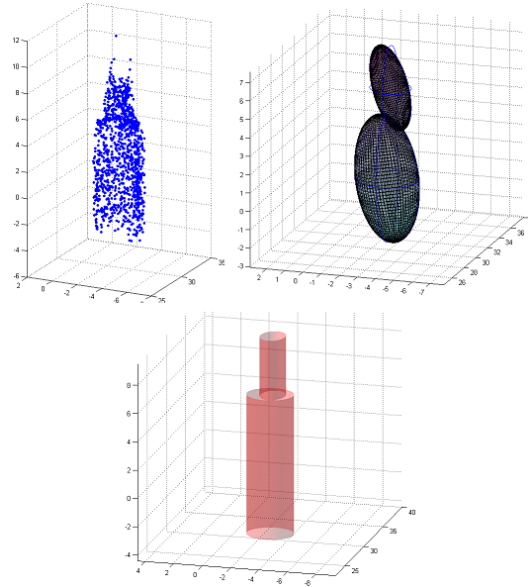


Figure 8. GMM generated from the 3D points obtained by grasp exploration and the recovered shape for the bottle.

Given the scale and rotation parameters and the means of each Gaussian (centroid), the cylinder shape was generated as shown in the figure 8.

As future work we intend to study and develop methods for 3D reconstruction using multimodality (data fusion). The main idea is to acquire visual cues from and data from grasp exploration to fuse them in a probabilistic volumetric map where each voxel has a probability of being occupied or not. One map for each sensor will be built and they will be updated on a global map by Bayesian filtering. To achieve this goal some preliminary steps are necessary, such as sensor calibration. We are starting this approach with preliminar results as presented in the next subsections. In the next subsections we describe

some works regarding dynamic background segmentation to assist removing the background of the image to facilitate the segmentation of the object, as well as method for sensors calibration to be possible reproject a set of 3D points from a frame of reference to another one. After these steps we intend adopt a probabilistic method for 3D reconstruction of the object for its characterization.

A. Dynamic Background Segmentation

We use the *horopter* concept in order to dynamically remove the background of the image. For that, the stereo camera has been calibrated. We used Bouguet toolbox [5] to acquire the homographic matrix between the cameras. This means that only objects inside the area are possible of being detected and when applying color to the 3D reconstruction we just need to consider a small amount of pixels instead of the whole image. Our approach is based on the *Geometric Horopter* and in order to calculate the horopter, first we obtain the stereo disparity map. Disparity map represents the difference of distances between points of a pair of images; meanwhile *depth maps* represents the expected depth/distance that an area is considered to be away from the camera.

We have used the Intel Open Source Computer Vision library [9] and an adaptation of the SVS [18] library in order to get the depth map. The SVS library first constructs a disparity space image from stereo image pair, and then calculates temporary disparity maps using the SAD method [7]. Later stage of the algorithm will reduce both the blurred errors at depth discontinuities and the mismatched errors at half occluded areas. The final step was to use a median filter to interpolate the dense disparity map. Once one has calibrated the cameras and the disparity map calculated, to obtain the depth map is trivial.

The Vieth-Muller Circle defines the region where the disparity is equal to zero, while the disparity grows for inside with positive values and grows (shrinks if considering the raw value) to outside with negative values. Pixels that present negative values for disparity, will be assigned zero value (black color pixels). The result is a segmented image where the pixels calculated to be inside the Vieth-Muller circle define the 'visible' objects within the circle. The segmented image (Fig.9) results in a region of interest and this region will define the true input pixels for the reprojection phase.

Notice that we still have some noise at the segmented images, these noisy areas usually exist due to homogeneous areas in the original image. Homogeneous areas and also very similar neighbor features of the image can add noise to our depth map and consequently to the final horopter segmented image.

B. Sensors Calibration

We performed a calibration between the Polhemus Liberty 240/8 tracking device and stereo camera to acquire a transformation to reproject the 3D points of the tracker device frame of reference in the image plane.



Figure 9. Horopter technique (left: original image; right: segmented image).

The stereo camera is mounted in a robotic head (Fig.10) and comprises two Guppy monocular cameras capable of vergence. The distance between the two cameras is 10cm. The first step of this calibration is to acquire the intrinsic and extrinsic parameters of the stereo camera. The Polhemus device gives us the 3D points related to its reference frame, thus we can use the strategy of using a white tape on the sensor (Fig.11) to recognize this "mark" in the left and right images to compute the 3D point. At least a set of 25 images are necessary. The 3D point from the tracker device sensor is acquired in the same instant of the images. The stereo camera and the tracker reference frames, $\{C\}$ and $\{P\}$ respectively, are rigid to each other. Initially the calibration is done keeping the cameras parallel and then the homographic matrix is updated at each time we move the vergence. Collecting two sets of 3D corresponding points in two coordinate references, ${}^c p = \{{}^c p_i | i = 1, \dots, N\}$ and ${}^p p = \{{}^p p_i | i = 1, \dots, N\}$ we can find the transformation of a 3D point in $\{P\}$, ${}^p p$ to $\{C\}$, ${}^c p$. To compute ${}^p R_c$ and ${}^p t_c$ (rotation and translation matrices of the homogeneous transformation) Arun's method described in [10] has been used which is based on an algorithm to find the least-squares solution of R and t (rotation and translations) using singular value decomposition (SVD). Fig. 12 shows that increasing the number of collected points from Polhemus and Camera reduce reprojection errors and increase the precision of the result. Its horizontal axis is for number of points used in the calibration, and the vertical axis indicates value of reprojection errors in the scale of pixel. For more details of the calibration method see [6].



Figure 10. Stereo vision consistent of two Guppy monocular cameras mounted in a robotic head .

Fig. 13 shows the reprojected points of the tracker device (acquired by the sensors on the fingertips) in the segmented image of the bottle.

VI. CONCLUSION

In this work a novel way of *object shape retrieval* by *grasp exploration* is presented. Using two electromagnetic tracker sensors, one on the index fingertip and another on the thumb



Figure 11. Right image acquired from stereo camera. The tracker sensor (with a white tape on it) is attached on a tripod for 3D point acquisition for calibration.

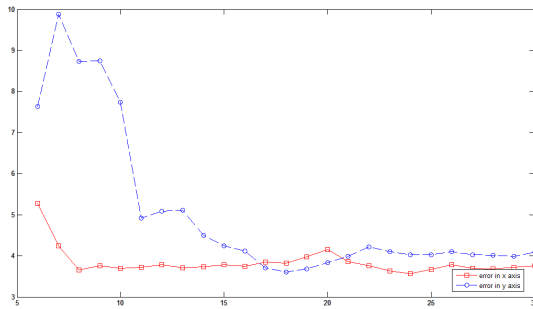


Figure 12. Number of used points in the calibration and the value of reprojection errors in the scale of pixel.

fingertip we could make movements around to the object to acquire raw data of its shape. GMM was used for clustering of the raw data to detect features (eigenvalues) to represent each shape (e.g. sphere, cylinder and plane). A probabilistic classification of the shapes primitives by using Bayesian techniques was proposed. Acquiring the features of each shape we computed histograms of possible shapes in a learning phase. Using the algorithm presented in [11] we could match the shape dispositions (cylinder, sphere and plane orientations and scale). As future work, we intend to use visual cues such as texture to characterize the object, as well as to obtain 3D reconstruction by using the 3D point cloud from different modalities (vision and grasp exploration). To achieve this goal sensors calibration is needed. We also presented the results of the calibration between the tracker device and stereo camera showing the reprojected points of the grasp exploration (Fig.13) on the segmented image acquired from horopter technique. The calibration step has shown satisfactory results and we can assume that will be possible to reconstruct the object shape using the 3D points acquired from stereo camera and grasp exploration. For the object (bottle of wine) used in our experiment the algorithm of shape retrieval easily recovered the cylinder shape for each one of the two Gaussians generated, as well as the scale in x , y , z axes and the rotation in Euler angles.

ACKNOWLEDGMENT

This work is partially supported by HANDLE project funded by the European Commission within the Seventh Framework Programme FP7 under grant agreement 231640. Diego Faria is supported by Portuguese Foundation for Science and Technology (FCT).

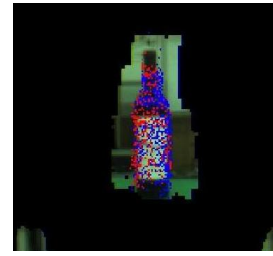


Figure 13. Reproject 3D Points of the tracker device in the image plane. Red color points represent were acquired from the thumb and the blue color points were acquired from the index finger.

REFERENCES

- [1] Polhemus liberty electromagnetic motion tracking system. <http://www.polhemus.com/>.
- [2] D. H. Ballard. Generalizing the hough transform to detect arbitrary shapes. *Pattern Recognition*, 13(2):111–122, 1981.
- [3] A. Bierbaum, Ilya Gubarev, and Rüdiger Dillmann. Robust shape recovery for sparse contact location and normal data from haptic exploration. *IEEE-RAS, International Conference on Humanoid Robots.*, 2008.
- [4] A. Blake. A symmetry theory of planar grasp. *The International Journal of Robotics Research*, 14:425–444, 1995.
- [5] Jean-Yves Bouguet. Camera calibration toolbox for matlab. <http://www.vision.caltech.edu/bouguetj/calibdoc/index.html>, 2006.
- [6] D. R. Faria, H. Aliakbarpour, and J. Dias. Grasping movements recognition in 3d space using a bayesian approach. In *Proceeding of The 14th International Conference on Advanced Robotics, ICAR'09. Munich, Germany. June, 2009*.
- [7] O. Faugeras, B. Hotz, H. Mathieu, T. Vieville, Z. Zhang, P. Fua and E. The ron, L. Moll, G. Berry, J. Vuillemin, P. Bertin, and C. Proy. Real time correlation-based stereo algorithm, implementations and application. Technical report, INRIA, Technical Report 2013, 1993.
- [8] W. Forstner and B. Moonen. A metric for covariance matrices. Technical report, Dpt. of Geodesy and Geoinformatics - University of Stuttgart, 1999.
- [9] Intel. Intel open source computer vision library. <http://www.intel.com/technology/computing/opencv/index.htm>, 2006.
- [10] T. S. Huang K. S. Arun and S. D. Blostein. Least-squares fitting of two 3-d point sets. 1987.
- [11] P. Nunez, P. Drews Jr, R. Rocha, M. Campos, and J. Dias. Novelty detection and 3d shape retrieval based on gaussian mixture models for autonomous surveillance robotics. In *to appear in Proceedings of The 2009 IEEE/RSJ International Conference on Intelligent Robots and Systems, IROS'09, St. Louis, MO, USA., 2009*.
- [12] P. Pekka, J. Ilonen J. K. Kamarainen, and H. Kälviäinen. Feature representation and discrimination based on gaussian mixture model probability densities-practices and algorithms. *Pattern Recogn.*, 39:1346–1358, 2006.
- [13] J.M. Iñesta P.J. Sanz and A.P. Del Pobil. Planar grasping characterization based on curvature-symmetry fusion. *Applied Intelligence*, 10:25–36, 1999.
- [14] Jorma Rissanen. *Information and Complexity in Statistical Modeling*. Springer Publishing Company Incorporated, 2007.
- [15] Ruwen Schnabel, Roland Wahl, and Reinhard Klein. Efficient ransac for point-cloud shape detection. *Computer Graphics Forum*, 26(2):214–226, June 2007.
- [16] Johan W. Tangelder and Remco C. Veltkamp. A survey of content based 3d shape retrieval methods. *Multimedia Tools Appl.*, 39(3):441–471, 2008.
- [17] J.S Gati P. Servos R.S. Menon T.W James, G.K Humphrey and M.A Goodal. Haptic study of three-dimensional objects activates extrastriate visual areas. *Neuropsychologia*, 40:1706–1714, 2002.
- [18] Videre. Videre design. <http://www.videredesign.com/>.
- [19] Miguel Vieira and Kenji Shimada. Surface mesh segmentation and smooth surface extraction through region growing. *Comput. Aided Geom. Des.*, 22(8):771–792, 2005.
- [20] L. Ni X. Markenscoff and C.H. Papadimitriou. The geometry of grasping. *The International Journal of Robotics Research.*, vol. 9, no. 1:61–74, 1990.